International Journal of Research and Development in Applied Science and Engineering (IJRDASE)
ISSN: 2454-6844

Dairy of Treatment Process for Water Treatment using Ceramic Membrane Filtration to Produce Water

Shahsikant Rajpoot, Anupam Kumar Gautam
Civil Engineering Department
MUIT, Lucknow,
anupamkumargautam12@gmail.com

Abstract: The performance of the ceramic membrane coating was investigated. The flux data were fitted into the standardpore blocking model (SPBM) and the complete pore plugging model (CPPM) to understand the fouling mechanism. The process found to fit with a minimum coefficient of regression, showing that the foulants retained on the pores were smaller compared to the size of pores of the membrane. The dissolved oxygen (DO) was found to increase. The improvement of the effluent quality in terms of chemical oxygen demand (COD), turbidity and DO signifies that the coated membrane leads to increase in the efficiency of submerged ceramic membrane bioreactors. Results were obtained with coated membrane was much better compared to uncoated membranes. Thus coating of membranes helps in achieving excellent quality of effluent water.

1. Introduction:

Over 1.1 billion people worldwide lack access to improved drinking water sources, and many more lack access to safe water as defined by the WHO risk-based Guidelines for Drinking Water Quality (10-6 Disability Adjusted Life Years per person per year) (WHO 2006; WHO 2004). Conventional piped water systems using effective treatment to deliver safe water to households may be decades away in much of the developing world, meaning that many of the poorest people must collect water outside the home and are responsible for managing (e.g., treating and storing) it themselves at the household level (Sobsey 2002). This gap in service is a serious public health issue and has been addressed in the Millennium Development Goals, which aim to halve, by 2015, the proportion of people without access to safe water in 2000 (UN 2000). Unsafe drinking water contributes to a staggering burden of waterborne disease in developing countries, borne primarily by the poor. Particularly susceptible are children, the elderly, and immuno-compromised individuals, who are most vulnerable to diarrheal and other waterborne infectious diseases.

In response to the persistent problems associated with waterborne diseases worldwide, new strategies for safe water provision are gaining currency, including treating drinking water at the household level to reduce the ingestion of pathogenic microbes. Taken together, devices that can be used to treat water and/or prevent contamination of stored water in the home are referred to as household water treatment (HWT) or point-of-use (POU) technologies. These comprise a range of options that can enable individuals and communities to reduce microbial pathogens or chemical contaminants in collected water at the point of use, usually at the household level. POU technology has the potential to fill the service gap where piped water systems are not possible, potentially resulting in substantial positive health impacts in developing countries (Sobsey 2006). Recent meta-analyses of field trials have suggested that household-based water quality interventions such as appropriate treatment and safe storage are effective in reducing diarrheal disease (Fewtrell et al. 2005; Clasen et al. 2006a, 2007).

2. Related Work:

An estimated 1.8 million people die every year from diarrheal diseases, less than AIDS (2.8 million) but more than tuberculosis (1.6 million) and malaria (1.3 million) (WHO 2004). The majority of deaths are associated with diarrhea among children under five years of age in developing countries, who are more susceptible to malnutrition, dehydration, or other secondary effects associated with these infections (WHO 2004). Taken together, diarrheal diseases are the third highest cause of illness worldwide and the third highest cause of death in children worldwide (WHO 2004). Most diarrheal illness is associated with unsafe water, sanitation, and hygiene (Prüss-Üstün et al. 2004). Prüss et al. (2002) estimated that 4.0% of all deaths and 5.7% of the global disease burden are attributable to inadequate water, sanitation, and hygiene, including diarrheal diseases and other water-related diseases such as ascariasis and schistosomiasis, claiming 4.2% of disability-adjusted-life years (61.9 million) worldwide (WHO 2004). The study of human health risks due to WSH-related pathogen exposure has been central to the field of environmental health for over 150 years (Snow 1855), although the current global burden of diarrheal disease suggests there is still progress to be made.

An unknown percentage of the diarrheal disease burden is due solely to unsafe drinking water, since the viral, bacterial, and parasitic microbes causing diarrheal disease may also be transmitted through contaminated food, hands, fomites, or other routes (Wagner and Lanoix 1958). Drinking water quality, however, does play an important role in the risk of diarrheal diseases in humans and access to safe water is a

major determinant of diarrheal disease outcomes. Diarrheagenic organisms generally originate in fecal matter and are transmitted through the fecal-oral route of infection (Curtis et al. 2000). Traditionally, among the most serious waterborne risks to public health have been the bacteria Shigella spp. (bacterial dysentery), Vibrio cholerae (cholera), and Salmonella spp. (typhoid, paratyphoid fever). Although these have mostly been eliminated from the developed world through advances in drinking water treatment, sanitation, and hygiene (Mackenbach 2007), they and other emerging and rëmerging pathogens continue to compromise water quality, and thus public health, in the less developed countries.

3. Methodology:

The silicon carbide ceramic membrane was procured from the BHEL. The composite materials synthesized, namely chitosan-activated carbon, cellulose acetate-activated carbon, PVA-sodium alginate-gelatin-ZnO, sodium alginate-gelatin-ZnO, nano zerovalent iron (nZVI), Ag-doped TiO2 nanoparticles, and sodium alginate-nZVI-bentonite, were subjected to the material characterization for understanding the morphology and chemical compositions of the composites. The SEM, energy-dispersive X-ray spectroscopy (EDS), TEM, FTIR, X-Ray Photoelectron Spectroscopy (XPS), BET surface analyzer were used for the characterization of the materials mentioned above.

A. Scanning Electron Microscopy (SEM)

The SEM employs the focused beam of electrons that react with the specific sample to construct a topological image and relative composition. The main components in the SEM include the electron source, the column which contains electromagnetic lenses, the sample chamber, the electron detector, and the computer display. The focused beam of an electron will produce secondary electrons (SEs), backscattered electrons, and characteristic X-ray, which is detected with respective detectors and finally displayed on the monitor.

Sample Preparation: Samples for testing were dried thoroughly to eliminate the traces of moisture and solvent, affecting the quality of the SEM images. The carbon tape was used to cover the specific slot in the specimen chamber on which the sample was attached firmly. The samples were coated using gold by employing low vacuum sputter coating, which increases the sample's conductivity and helps to obtain superior quality SEM images. The sample coated was placed over the specific slot and locked into the chamber. A field emission gun-scanning electron microscope (FEG-SEM): JEOL JSM-7600F located at the Sophisticated Analytical Instrumental Facility (SAIF) at Indian Institute of Technology, Bombay (IITB) and SEM of BMS College of Engineering were used during the project.

B. Energy Dispersive X-ray (EDX) Spectroscopy

The EDX spectroscopy is primarily used in the elemental composition detection of the materials by employing SEM. The EDX detects elements that have an atomic number higher than that of boron. The elements can be detected at a concentration of at least 0.1%. The application of EDX also includes identification and material evaluation, contamination, quality control screening, spot detection analysis of regions up to 10 cm in diameter, etc.

C. Transmission Electron Microscopy (TEM)

A transmission electron microscope (TEM) is similar to an ordinary optical microscope, except that a beam of electrons and electromagnetic lenses are replacing light and optical lenses. An electron source forms a stream of 100-400 keV electrons directed towards the specimen by applying a positive potential. While passing through a condenser system, the stream is focused and confined by metal apertures and magnetic lenses into a thin, focused and monochromatic beam. This beam then hits the surface where it is transmitted, diffracted, backscattered, or induces photoelectrons, x-ray fluorescence, or Auger electrons. The transmitted electrons form a two-dimensional projection of the sample, depending on the density and thickness, magnified by electron optics and depicted by a so-called bright field image. When analyzing the diffracted beams, the resulting dark-field images contain additional crystallographic information about the specimen.

Sample preparation: Samples for testing were dried thoroughly to eliminate the traces of moisture and solvent, affecting the quality of the TEM images. The carbon tape was used to cover the specific slot in the specimen chamber on which the sample was attached firmly. TEM images and selected area electron diffraction (SAED) patterns were collected using a JEOL JFM-2100F TEM operating at 200 kV located at SAIF IITB. Samples for these measurements were prepared by dropping a small volume of sonicated powders in ethanol onto a carbon-coated copper grid.

D. Fourier Transform Infrared Spectroscopy (FTIR)

Fourier transform spectrophotometer provides the IR spectrum swiftly compared to the other spectrophotometers. The instrument builds a beam of IR irradiation from a glowing black-body source. The beam of IR is led to pass through the interferometer where the spectral encoding occurs. The recombination of the IR beams with a difference in path lengths in the interferometer leads to constructive and destructive interference called an interferogram. The beam enters the samples compartment, and the sample absorbs specific frequencies of energy, which are uniquely characteristic of the sample from the interferogram. Then, the detector measures the special interferogram signal in energy versus time for all frequencies simultaneously. In the meantime, a beam is superimposed to provide a reference (background) for the instrument operation. Finally, the desirable spectrum was obtained after the interferogram automatically subtracted the background spectrum from the sample spectrum by Fourier transformation computer software.

Sample Preparation: Infrared spectroscopic measurements were performed on a Nicolet 6700 FTIR spectrometer

(Thermo Electron Corporation, USA; DTGS detector; KBr beamsplitter) located at IIT Bombay and FTIR in Chemical Engineering Department, MSRIT. For preparing KBr pellets, the sample was powdered and pressed in a pellet (200 mg; diameter 13 mm) at up to 7 MPa. Spectra were collected in the transmittance mode with a total of 64 scans (resolution 2 cm-1) and manipulated using the OMNIC (version 8.2.0.387) software supplied by the spectrometer manufacturer. All spectra were smoothed using the standard "automatic smooth" function of the software, which uses the SavitskyeGolay algorithm (95-point moving second-degree polynomial), and then the baseline was corrected using the "automatic baseline correct" function.

E. X-Ray Diffraction (XRD)

X-ray diffraction is a useful characterization technique that gives information about crystals and thin films' physical properties and structural aspects. The scattered intensity of the X-ray beam is produced by hitting the sample is carefully measured as a function of incident angle, scattered angle, polarization, and wavelength as described by Hull. Thus, XRD patterns act as a unique fingerprint of the material. The sample is mounted on a goniometer and rotated with a simultaneous bombardment of X-rays in the XRD machine. The X-rays on hitting the sample diffracts into different angles to produce two-dimensional images at different positions. This data is integrated to get three-dimensional data using the mathematical method of Fourier transform, combined with the chemical data of the sample. Although scattering of beams from the sample leads to destructive interference, there are specific directions in which they add up to give a diffraction pattern governed by Bragg's Law and is given by:

$$2d \sin\theta = n\lambda$$

where, θ is the incident angle, d is the spacing between the planes, n is an integer, and λ is the wavelength of the incident beam.

Sample Preparation: The samples subjected to XRD analysis were dried for up to 10 h before testing to eliminate the small amount of moisture and solvent to avoid generating distorted patterns. The samples were placed in the sample slot to make a powder bed, and the surface of the powder was smoothened. Testing all the samples was carried out by directly placing the coated surface upside inside the sample slot in the equipment without powdering the sample. The synthesized samples were subjected to X-ray diffraction in 2θ angles ranging from 5° to 80° with a step size of 0.05° and scanning rate of 1° per minute. X-ray diffraction machine employed for the present project purpose was a PANalytical Empyrean diffractometer equipped with the graphite monochromatized Cu-Kα radiation (λ=1.5406 Å) located at IITB and XRD at BMS College of Engineering Bangalore.

F. Pore Size Measurements

The adsorption and desorption phenomena of nonreactive gas on the solid surface is used to analyse the various physical factors affected by the formation of pores. Pressure is the prominent parameter in this technique. The gas such as nitrogen in the liquid state, fills the pores until the pressure reaches the saturation state. The amount of gas at the saturation state provides the total pore volume of the material. This approach is used widely, which is pioneered by Brunauer et al. and Barret et al. through their approach to the so-called Brunauere-Emmette-Teller (BET) and Barrette-Joyner-Halenda (BJH) surface area calculation. The researchers used this method in characterizing their samples for various applications. Using the behaviour of adsorption-desorption of N2 gas, various tools/machines have been invented to study porosity. Typically, samples were crushed into smaller pieces and degassed approximately for 4 h at 65 ℃ (338 K). The degassing step is inevitable to eliminate the moisture and impurities in the inner surface of the membrane. This process was followed by an analysis of the degassed sample, which is typically carried out overnight.

Sample Preparation: The samples tested for the surface area were subjected to drying at 100 ℃ for 3 h before outgassing. The samples were degassed at 150 ℃ for 90 min. The 3Flex BET surface area analyzer from Micromeritics instrumental corporation was used for characterization, which is located at IITB.

G. X-Ray Photoelectron Spectroscopy (XPS)

X-ray photoelectron spectroscopy, also known as electron spectroscopy for chemical analysis, is employed to test and understand the surface chemistry of the materials after an applied treatment such as fracturing, cutting, or scraping. XPS is the widely adopted tool for characterization of the material's surface because XPS can be applied to various materials and gives precise information on the quantitative and chemical state from the material's surface under analysis. The average depth of analysis for an XPS measurement is approximately 5 nm. Spatial distribution information can be obtained by scanning the micro-focused X-ray beam across the surface of the sample. In addition, depth distribution information can be obtained by combining XPS measurements with ion milling (sputtering) to characterize thin-film structures. The information from XPS provides about surface layers or thin-film structures is vital for many industrial and research applications.

Sample Preparation: The samples were powdered and dried in the vacuum and later mounted on the grid with adhesive tape. Monochromatic (Al Kα) X-ray source (600 W) with a pass energy of 20 eV and resolution of ~ 0.5 eV was used for the high-resolution scans, whereas 160 eV pass energy and ~ 2 eV resolution was used for the survey scans. The high-resolution XPS spectra of Ag 3*d*3/2 and Ag 3*d*5/2 were deconvoluted into separate components after subtracting the Shirley background and applying a 30% mixed Gaussian-Lorentzian peak shape function. Before the deconvolution, binding energies were corrected for the surface charge using the adventitious carbon C 1*s* spectra line (C-C) at the binding

energy of 284.8 eV, which was determined after deconvoluting the high-resolution C 1s peak. Kratos analytical Axis supra XPS located at IITB was used in this study.

4. Result and Discussion:

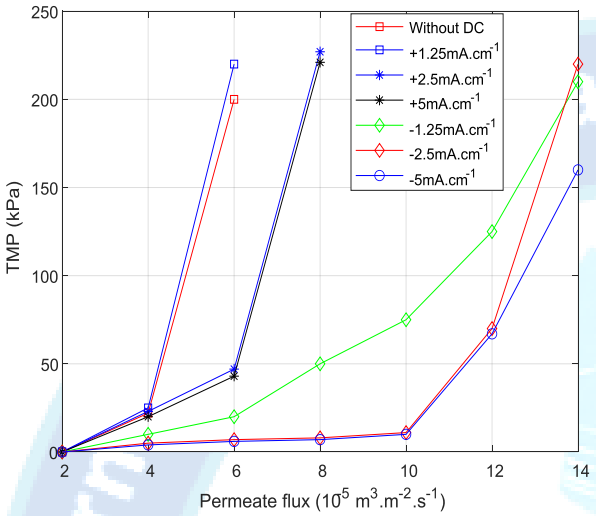

Figure 1. (a) TMP and flux profiles of membrane filtration with S. dimorphus of 0.05 g·L^{-1} under an initial permeate flux of 2.08 × 10^{-5} m^3·m^{-2}·s^{-1} in the cross-flow filtration test with different applied dc current densities. (b) TMP vs permeate flux for REM filtration. The red arrow shows the possible critical flux at 4.17 × 10^{-5}, 6.25 × 10^{-5} and 12.48 × 10^{-5} m^3·m^{-2}·s^{-1}.

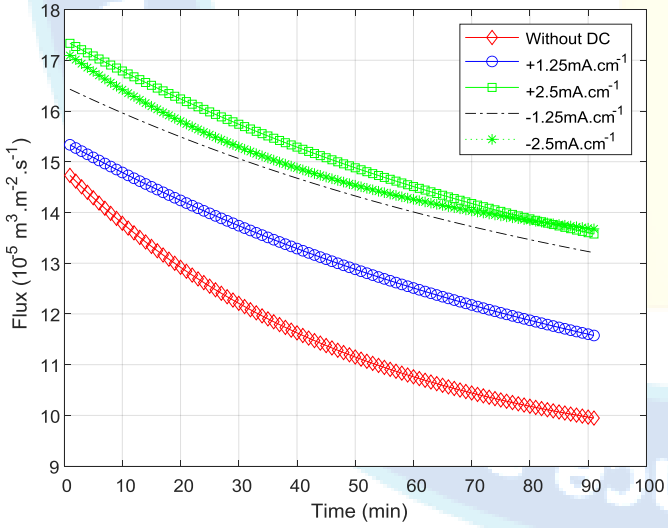

Figure 2 (a) Variations in permeate flux under a constant TMP of 68.9 kPa (10 psi) during continuous filtration with different dc current densities (algal concentration in the influent: 0.05 g·L-1).

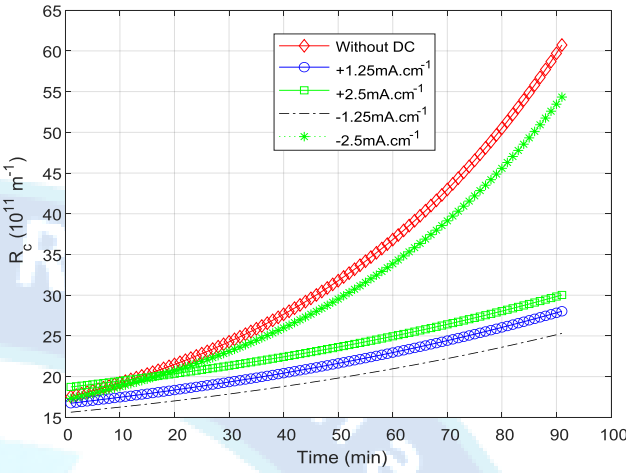

(b)Cake layer resistance (Rc) increase in the membrane filtration process with different dc current densities over 40 min time period.

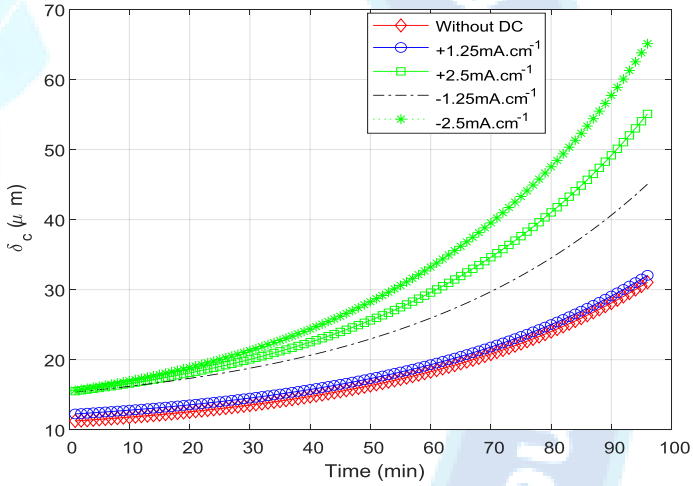

(c) Calculated cake layer thickness (δc) increase over time of filtration.

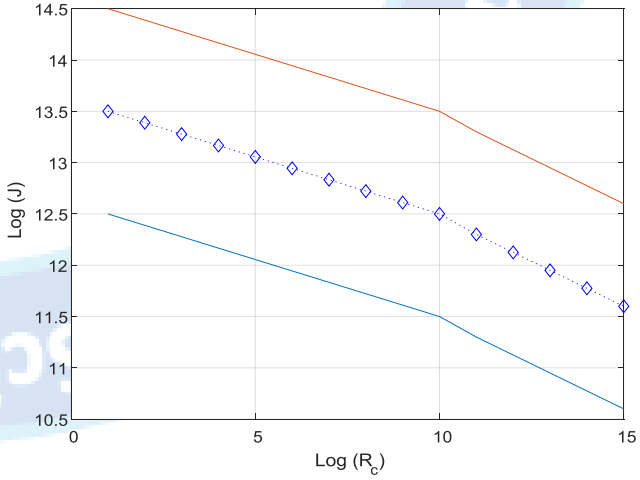

Figure 3. Plot of log(Rc) and log(J) under different positive/negative dc conditions. The purple and red dotted lines are the upper and lower limits of the plot, when

considering a relative error of 30% for the results of Rc as estimated from Figure 2.

5. Conclusion:

The presented resistance-in-series model calculations is proven to be a useful tool for computing and even predicting the dynamic increase of cake layer resistance (Rc) and thickness. Moreover, the model results better unravel the effects of electrochemical reactions on membrane filtration and fouling mitigation processes. For instance, the algal cake layer thickness and compressibility could both be affected by the anodic or cathodic reactions on electrochemical membranes. Overall, this study provides a new insight into the antifouling membrane filtration in algal separation and makes broader impacts on many other bioseparation or water treatment processes.

References:

[1] C Brepols, Sustainable adoption and future perspectives for membrane bioreactor applications, In Current Developments in Biotechnology and Bioengineering, 2020, pp. 205-233.
[2] AK Biswas, Water for sustainable development in the 21st century: a global perspective, International Journal of Water Resources Development, vol. 7, 1991, pp. 219-24.
[3] R Martin-Nagle, Fossil aquifers: a common heritage of mankind, Geo. Wash. Journal of Energy & Environmental Law, Vol. 2, 2011.
[4] C Niemitz, The present ecological situation of mankind–analysis and consequences, Anthropologischer Anzeiger, vol. 76, 2018, pp. 275-92.
[5] AD Patwardhan, Industrial Wastewater Treatment, PHI Learning Pvt. Ltd, 2017.
[6] Goswami L, Kumar RV, Pakshirajan K, Pugazhenthi G, A novel integrated biodegradation—microfiltration system for sustainable wastewater treatment and energy recovery, Journal of Hazardous Materials, vol. 365, 2019, pp. 707-15.
[7] Romani A, Michelin M, Domingues L, Teixeira JA, Valorization of wastes from agrofood and pulp and paper industries within the biorefinery concept: southwestern Europe scenario, Waste Biorefinery , 2018, pp. 487-504.
[8] Guerreiro RC, Jeronimo E, Luz S, Pinheiro HM, Prazeres AR, Cheese manufacturing wastewater treatment by combined physicochemical processes for reuse and fertilizer production, Journal of Environmental Management, vol. 264, 2020, pp. 110470.
[9] Meabe E, Lopetegui J, Ollo J, Lardies S, Ceramic Membrane Bioreactor: potential applications and challenges for the future, In Proceedings of the MBR Asia International Conference, Kuala Lumpur, Malaysia , 2011, pp. 25-26.
[10] Amin SK, Roushdy MH, Abdallah HA, Moustafa AF, Abadir MF, Preparation and characterization of ceramic nanofiltration membrane prepared from hazardous industrial Waste, International Journal of Applied Ceramic Technology, vol. 17, 2020, pp. 162-74.
[11] Sarkar B, Chakrabarti PP, Vijaykumar A, Kale V, Wastewater treatment in dairy industries- possibility of reuse, Desalination, vol. 195, 2006, pp. 141-52.
[12] Abdulgader M, Yu QJ, Zinatizadeh AA, Williams P, Rahimi Z, Performance and kinetics analysis of an aerobic sequencing batch flexible fibre biofilm reactor for milk processing wastewater treatment, Journal of Environmental Management, vol. 255, 2020, pp. 109793
[13] Bortoluzzi AC, Faitao JA, Di Luccio M, Dallago RM, Steffens J, Zabot GL, Tres MV, Dairy wastewater treatment using integrated membrane systems, Journal of Environmental Chemical Engineering, vol. 5, 2017, pp. 4819-27.
[14] Ganju S, Gogate PR, A review on approaches for efficient recovery of whey proteins from dairy industry effluents, Journal of Food Engineering, vol. 215, 2017, pp. 84-96.
[15] Ahmad T, Aadil RM, Ahmed H, ur Rahman U, Soares BC, Souza SL, Pimentel TC, Scudino H, Guimaraes JT, Esmerino EA, Freitas MQ, Treatment and utilization of dairy industrial waste: A review, Trends in Food Science & Technology, vol. 88, 2019, pp. 361-72.
[16] Mohan SS, Sheena KN, Dairy Waste Water Treatment Using Coconut Shell Activated Carbon and Laterite as Low Cost Adsorbents, International Research Journal of Engineering and Technology, vol. 6, 2019, pp. 306-309.
[17] Al-Jabari M, Iqefan N, Zahdeh N, Dweik H, Adsorption of organic pollutants from dairy wastewater on soil: pollution problem and control, International Journal of Global Environmental Issues, vol. 6, 2017, pp. 149-61.
[18] Lansing S. L and Martin J, Use of an ecological treatment system (ETS) for removal of nutrients from dairy wastewater, Ecological Engineering, vol. 28, 2006, pp. 235-245.
[19] M Sengil I A and ozacar, Treatment of dairy wastewaters by electrocoagulation using mild steel electrodes, Journal of Hazardous Materials, vol. 137, 2006, pp. 1197–1205
[20] Demirel B, Yenigun O and Onay T. T, Anaerobic treatment of dairy wastewaters: a review, Process Biochemistry, vol. 40, 2005, pp. 2583–2595.
[21] Balannec B, Vourch M, Rabiller-BaudryM, Chaufer B, Comparative study of different nanofiltration and reverse osmosis membranes for dairy effluent treatment by dead-end filtration, Separation and Purification Technology, vol. 42, 2005, pp. 195-200.
[22] Vourch M, Balannec B, Chaufer B, Dorange G, Nanofiltration and reverse osmosis of model process waters fromthe dairy industry to produce water for reuse, Desalination, vol. 172, 2005, pp. 245–256.